OAK RIDGE
NATIONAL LABORATORY
MANAGED BY UT-BATTELLE
FOR THE DEPARTMENT OF ENERGY

ORNL/TM-2007/040

Engineering Science and Technology Division

Enclosure Requirements to Protect Personnel from Spinning Rotor Failures at the Power Electronics and Electric Machinery Research Center

John W. McKeever

Publication Date: August 2007

Prepared by the
OAK RIDGE NATIONAL LABORATORY
Oak Ridge, Tennessee 37831
managed by
UT-BATTELLE, LLC
for the
U.S. DEPARTMENT OF ENERGY
Under contract DE-AC05-00OR22725

UT-BATTELLE
ORNL-27 (4-00)

DOCUMENT AVAILABILITY

Reports produced after January 1, 1996, are generally available free via the U.S. Department of Energy (DOE) Information Bridge:

Web site: http://www.osti.gov/bridge

Reports produced before January 1, 1996, may be purchased by members of the public from the following source:

National Technical Information Service
5285 Port Royal Road
Springfield, VA 22161
Telephone: 703-605-6000 (1-800-553-6847)
TDD: 703-487-4639
Fax: 703-605-6900
E-mail: info@ntis.fedworld.gov
Web site: http://www.ntis.gov/support/ordernowabout.htm

Reports are available to DOE employees, DOE contractors, Energy Technology Data Exchange (ETDE) representatives, and International Nuclear Information System (INIS) representatives from the following source:

Office of Scientific and Technical Information
P.O. Box 62
Oak Ridge, TN 37831
Telephone: 865-576-8401
Fax: 865-576-5728
E-mail: reports@osti.gov
Web site: http://www.osti.gov/contact.html

This report was prepared as an account of work sponsored by an agency of the United States Government. Neither the United States government nor any agency thereof, nor any of their employees, makes any warranty, express or implied, or assumes any legal liability or responsibility for the accuracy, completeness, or usefulness of any information, apparatus, product, or process disclosed, or represents that its use would not infringe privately owned rights. Reference herein to any specific commercial product, process, or service by trade name, trademark, manufacturer, or otherwise, does not necessarily constitute or imply its endorsement, recommendation, or favoring by the United States Government or any agency thereof. The views and opinions of authors expressed herein do not necessarily state or reflect those of the United States Government or any agency thereof.

TABLE OF CONTENTS

LIST OF FIGURES

LIST OF TABLES

INTRODUCTION

Performance evaluation of electric motors is a major function of the Power Electronics and Electric Machinery Research Center (PEEMRC). Normally these motors have a fixed wire-wound stator and a rotating rotor, which may have conductors embedded in a ferromagnetic core (induction motors), magnets mounted on the surface of the ferromagnetic core with a thin metal or composite cylinder or ring to hold them in place, or magnets embedded in the ferromagnetic core. Most of the work currently involves the last two permanent magnet (PM) configurations.

Although the stator of a radial-gap motor can absorb energy from many of the fragments ejected from the rotor during operation, the stator of an axial-gap motor is not positioned to provide significant protection. The housing of each motor can also absorb some of the energy. The most conservative approach, however, is to assume that all fragments from the rotor must be contained by a protective enclosure. An ideal enclosure is transparent. Manufacturers of such plastics as Lexan, Tuffak, and Cyrolon sell different variations of transparent enclosure material. Lexan is a polycarbonate sheet. Lexgard® is a penetration resistant material made by layering polycarbonate material between pieces of ordinary glass. A fragment striking a sheet of enclosure material will pierce the surface layer, but the layered polycarbonate-glass material is able to absorb the fragment's energy before it completes penetration. Tuffak® is Lexan polycarbonate. Cyrolon® bullet resistant material is acrylic sheet.

The ability of the enclosure to stop a fragment depends on its thickness as well as the penetration capability of the fragment; for example, a lead fragment has much less penetrating capability than a steel fragment. Enclosure thicknesses are commercially available to provide several levels of protection. These levels depend on the momentum of the fragments and have been evaluated for some common types of ammunition.

This summary quantifies four typical worst-case fragments which have maximum translational kinetic energy when ejected from a rotating annulus.

1. The first fragment is released from a rotating annular titanium ring.
2. The second fragment is a magnet released from the Oak Ridge National Laboratory's (ORNL's) 30-kW axial-gap PM motor. Analysis of the second fragment which is like a segment of half-angle, α, from a thin annular ring is similar to that of the titanium ring segment except that the angle is 10° instead of 133°.
3. The third fragment is a magnet from the radial-gap 6-kW fractional-slot surface-mounted PM (SPM) motor with concentrated windings. Analysis of the third fragment is similar to the analysis of the second fragment.
4. The fourth fragment is a 133° segment of an entire rotor which assumes that the laminates and magnets in the rotor fail as a single fragment, truly a worst case assumption.

MAXIMUM KINETIC ENERGY SEGMENT OF AN ANNULAR RING

Upon release, the center of mass of this fragment, which is an annular segment in this analysis, translates along a path perpendicular to the radius at which it was released until it strikes the enclosure. As it translates, it continues to rotate about its center of mass at an angular velocity equal to its rotational velocity at the instant of release. The kinetic energy that the angular segment had the instant before release is the sum of the translational and rotational kinetic energies the instant after release. Figure 1 is a sketch of a general annular segment being considered. The length, L, of the segment is perpendicular to the sketch. The value of α is chosen so that the translational velocity of the segment is a maximum.

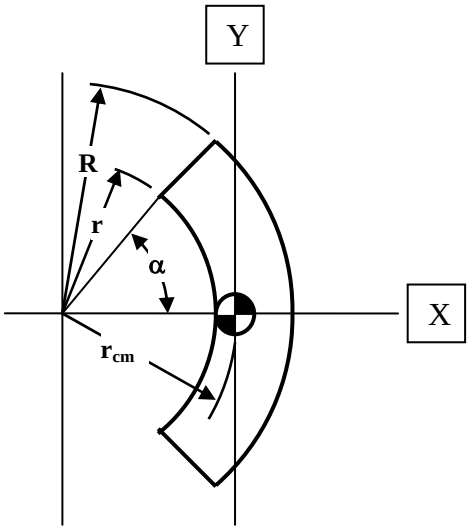

Fig. 1. Segment whose translational kinetic energy must be contained.

A titanium ring is used to maintain proper radial interference between the magnets of ORNL's 18-pole axial-gap rotor and the aluminum hub. If the titanium ring fails annular segments with half-angle, α, may be ejected at a velocity, $v = \omega r_{cm}$, where ω is the angular velocity in radians/s and r_{cm} is the radius of the center of mass of the segment given by the equation,

$$r_{cm} = \frac{2\sin(\alpha)\left(R^3 - r^3\right)}{3\alpha\left(R^2 - r^2\right)} \quad . \tag{1}$$

In Eq. (1), R and r are the outer and inner radii, respectively, of the annulus.

The mass in lb_m and the momentum in lb_fs of the segment are given by the equations

$$m = \rho\left(R^2 - r^2\right)L\alpha\,, \tag{2}$$

and

$$p = m\omega r_{cm} = \frac{2\rho\omega L\sin(\alpha)\left(R^3 - r^3\right)}{3g_o}\,, \tag{3}$$

where ρ is the density of the annular ring, $lb_m/in.^3$,
α is the half-angle of the annular segment, radians,
L is the thickness of the annulus, in., and
g_o is the gravitational constant, 386 $(lb_m\text{-in.})/(lb_f\text{-}s^2)$.

The kinetic energy of the fragment in in-lb_f is

$$T = \frac{p^2}{2m} = \frac{2}{9}\frac{\rho\omega^2 L}{g_o}\frac{\left(R^3 - r^3\right)^2}{\left(R^2 - r^2\right)}\frac{\sin^2(\alpha)}{\alpha} \ . \tag{4}$$

To find the value of α for the segment with maximum kinetic energy we derive $\frac{dT}{d\alpha} = 0$ and solve for α_{max}. This leads to the equation

$$\frac{dT}{d\alpha} = f(\rho,\omega,R,r,L)\left[\frac{\alpha 2\sin\{\alpha\}\cos\{\alpha\} - \sin^2\{\alpha\}}{\alpha^2}\right] = 0 . \tag{5}$$

Equation (5) will be zero if the numerator of the term in square brackets is zero producing the transcendental equation for α_{max}

$$2\alpha_{max} = \tan(\alpha_{max}) \ . \tag{6}$$

The solution of Eq. (6) is $\alpha_{max} = 1.165561186$ radians corresponding to 66.78173°. Since the angle is half the fragment, the maximum kinetic energy fragment is 133.56°. Evaluation of $\frac{d^2T}{d\alpha^2}$ at α_{max} is negative confirming that T is a maximum. For this fragment, the value of $\frac{\sin^2(\alpha_{max})}{\alpha_{max}}$ is 0.724611352 which leads to the equation for a fragment's maximum kinetic energy

$$T_{max} = 5.75705x10^{-4}\,\rho\omega^2 L\frac{\sin^2(\alpha)}{\alpha}\frac{\left(R^3 - r^3\right)^2}{\left(R^2 - r^2\right)} = 4.17163x10^{-4}\,\rho\omega^2 L\frac{\left(R^3 - r^3\right)^2}{\left(R^2 - r^2\right)} \ . \tag{7}$$

MAXIMUM ENERGY CALCULATION FOR THE TITANIUM RING IN ORNL'S 30 KW AXIAL-GAP PM ROTOR

This rotor is being rotated in several projects. For the annular ring, which girdles the magnets and maintains proper interference, the parameters are

ρ is the density of titanium, 0.16 $lb_m/in.^3$,
ω is the speed in radians per second ($\omega = \Omega_{rpm}\frac{2\pi}{60}$),
L is the thickness of the ring, 0.2 in.,
R is the outer radius of the annulus, 5.6 in.,
r is the inner radius of the annulus, 5.0 in., and
a is the maximum kinetic energy half-angle, 66.78173° or 1.165561186 radians.

The upper curve in Fig. 2(a) shows the maximum translational kinetic energy of a titanium ring fragment whose center of mass is moving toward the wall of the enclosure. The curve below it is the corresponding rotational kinetic energy of that fragment about its center of mass. The enclosure must be designed to withstand the translational impact of the fragment and to absorb any machining action that occurs from the rotating fragment. Figure 2(a) is for lower speed analysis. Figure 2(b) is for higher speed analysis.

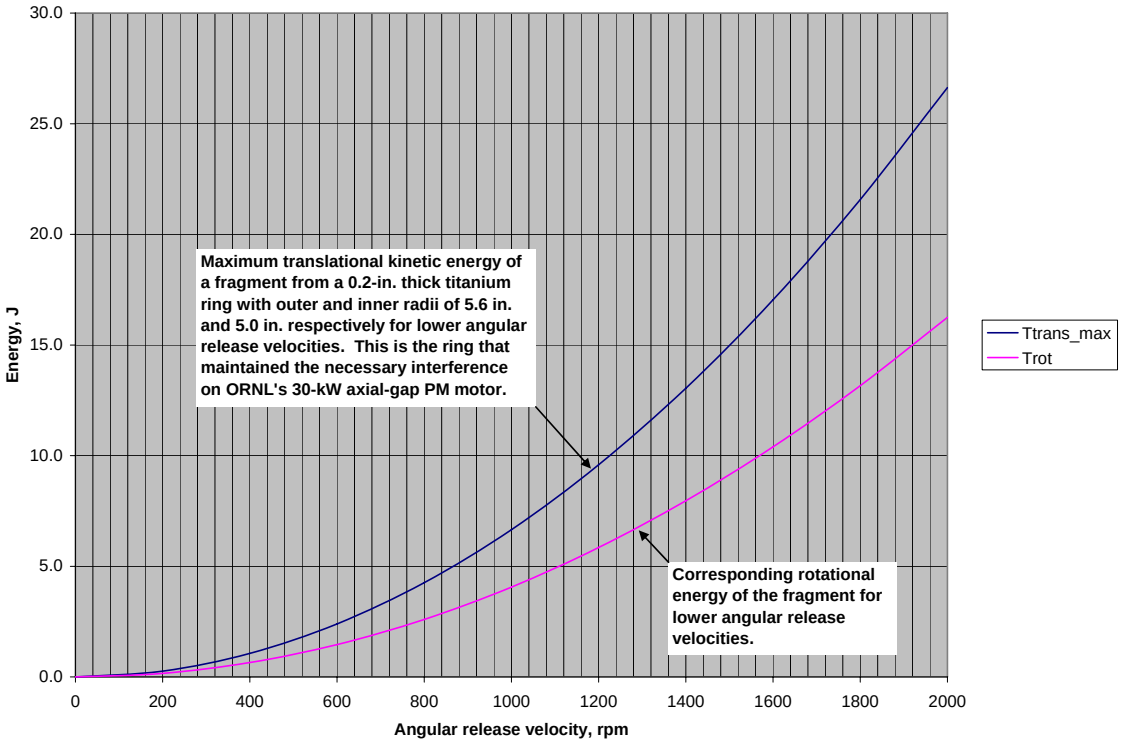

Fig. 2(a). Maximum kinetic energy fragment from a titanium ring released over a low speed range.

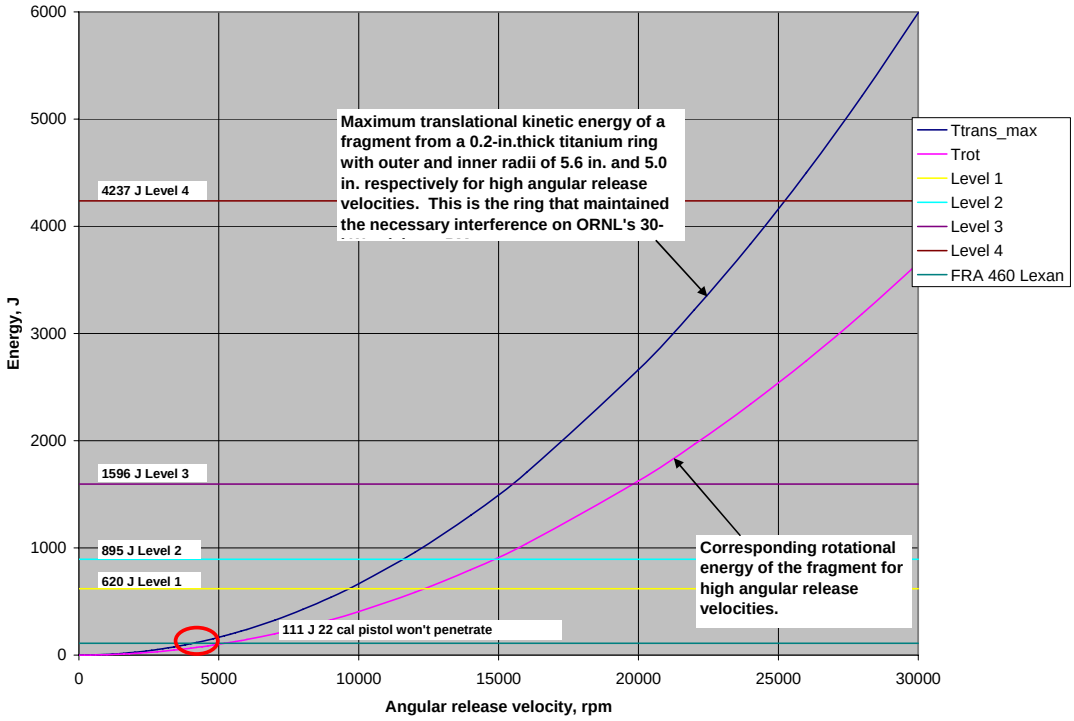

Fig. 2(b). Maximum energy of a titanium ring fragment released over a high speed range.

Four levels of protection provided by polycarbonate laminate products are shown. Laminates have been rated per *Underwriters Laboratory UL 752 Standard Bullet Resisting Equipment*, 9th Edition, January 27, 1995. Table 1 summarizes some products recommended to provide protection for each level. These materials have no ballistic ratings in and of themselves but are to be used as components in systems including laminated safety glass and appropriate air spaces to achieve specific ballistics ratings.

Table 1. Comparative levels of bullet resistance

Level	Projectile type	Projectile mass, g	Maximum velocity, ft/s	Kinetic energy, J	Products
Lexan Safe	22 cal slug fired from a pistol does not penetrate 1/2-in. thick Lexan.	2.6	960	111	FRA 460 Lexan
Lexan Unsafe	22 cal slug fired from a rifle **penetrates** 1/2-in. Lexan.	2.6	1200	173	Needs more than 1/2-in. FRA 460 Lexan
URL-752 1	9-mm dia. bullet fired from medium power small arms automatic at a range of 15 feet (4.6 meters).	8	1293	620	Acrylite BRT 1.25" HYGARD BR750 Lexgard 1
URL-752 2	0.357- in. dia. bullet fired from high power small arms, Magnum	10.2	1375	895	Acrylite BRT 1.378" HYGARD BR1000
URL-752 3	0.44-in. dia. Bullet fired from super power small arms, Magnum	15.6	1485	1596	Acrylite BRT 1.25" HYGARD BR-1250 Lexgard 3

The PEEMRC uses 1/2-in. thick Lexan polycarbonate sheets as the walls of enclosures to protect personnel from failing semiconductors or other small energy releases. Occasions will arise when the test cells are occupied and our ability to meet tight schedules will depend upon being able to operate motors in the laboratory outside the test cells at low speeds. Charles Mulcahy, who is in charge of physical testing at General Electric Plastic Extrusions (GE), provided information about Lexan that brackets its penetration resistance. The GE product, FRA 460, has been specifically tailored to meet the Federal Railway Administration (FRA) specifications for windows in passenger cars. The specification is that the window may not be penetrated by a 22 caliber slug shot from a pistol. Mr. Mulcahy explained that the slug mass is 40 grains and that when shot from a pistol its exit speed is 960 ft/s. This produces a kinetic energy of 111 J. When the same slug is fired from a rifle so that its exit velocity is 1200 ft/s, it produces a kinetic energy of 173 J, which does penetrate the FRA 460. Lexan product FRA-460 can protect against penetration by fragments with energy at or below 111 J.

ENERGY CALCULATION FOR AN EJECTED AXIAL-GAP MAGNET

This is the approximate wedge shaped magnet found in ORNL's 30-kW axial-gap PM motor. For magnet's parameters are

ρ is the density of steel, 0.28 $lb_m/in.^3$,

ω is the speed in radians per second ($\omega = \Omega_{rpm} \frac{2\pi}{60}$),

L is the thickness of the ring, 0.2 in.,

R is the outer radius of the annulus, 5.0 in.,
r is the inner radius of the annulus, 3.4 in., and
α is the magnet's half-angle, 10^{o} or 0.1745 radians.

The upper curve in Fig. 3(a) shows the translational kinetic energy of a magnet whose center of mass is moving toward the wall of the enclosure. The curve below it is the corresponding rotational kinetic energy of that fragment about its center of mass. Figure 3(a) is for lower speed analysis. Figure 3(b) is for higher speed analysis.

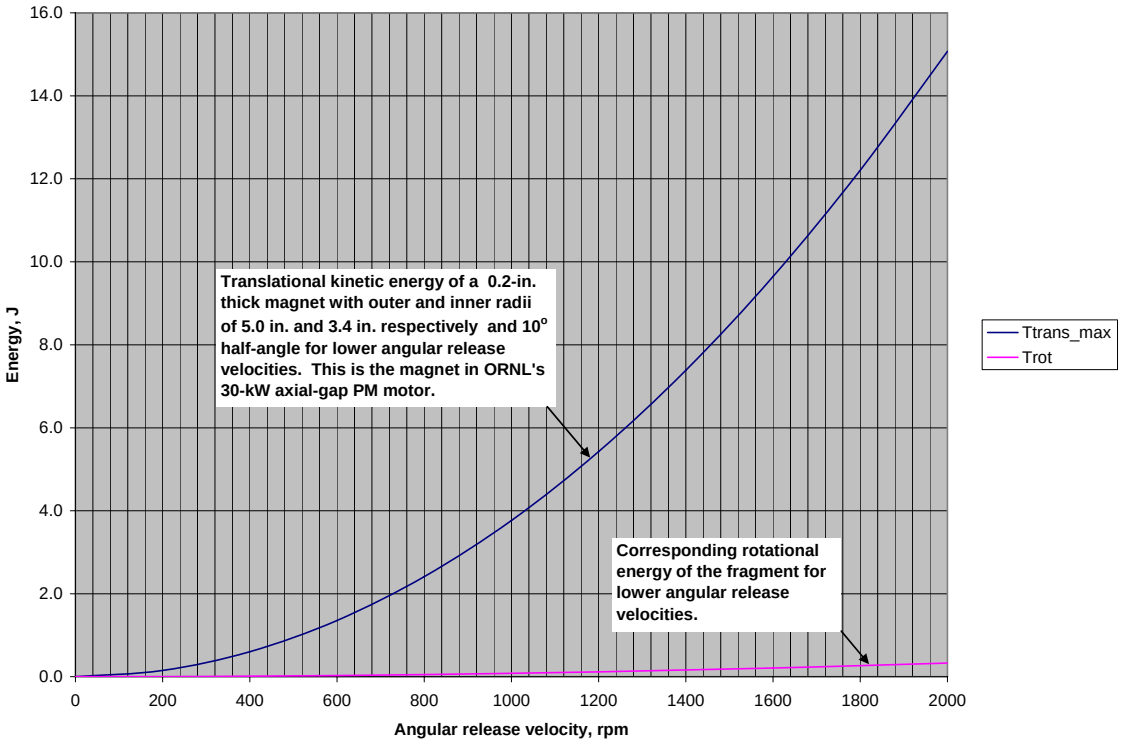

Fig. 3(a). Translational energy of an axial-gap magnet released over a low speed range.

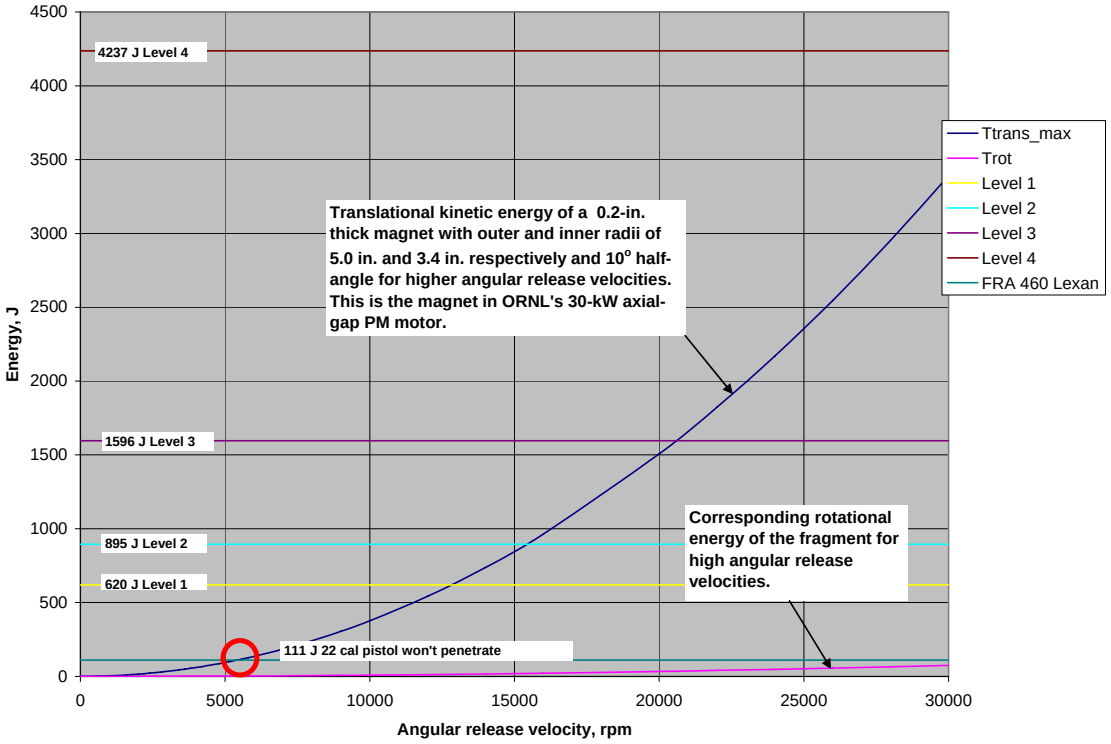

Fig. 3(b). Translational energy of an axial-gap magnet released over a high speed range.

ENERGY CALCULATION FOR A MAGNET EJECTED FROM THE 6-KW RADIAL-GAP FRACTIONAL-SLOT SPM MOTOR WITH CONCENTRATED WINDINGS

This is the circumferentially segmented magnet on the rotor of the 6-kW fractional slot concentrated windings (FSCW) SPM motor designed and tested by the University of Wisconsin in Madison (UWM) and used at ORNL to evaluate a control scheme. Each magnet's parameters are

ρ is the density steel, 0.28 $lb_m/in.^3$,

ω is the speed in radians per second ($\omega = \Omega_{rpm} \frac{2\pi}{60}$),

L is the thickness of the ring, 2.362 in.,
R is the outer radius of the annulus, 4.0 in.,
r is the inner radius of the annulus, 3.488 in., and
α is the magnet's half-angle, 5.7^o or 0.09948 radians.

The upper curve in Fig. 4(a) shows the translational kinetic energy of a magnet released from the 6-kW FSCW SPM motor, whose center of mass is moving toward the wall of the enclosure. The curve below it is the corresponding rotational kinetic energy of that fragment about its center of mass. Figure 4(a) is for lower speed analysis. Figure 4(b) is for higher speed analysis.

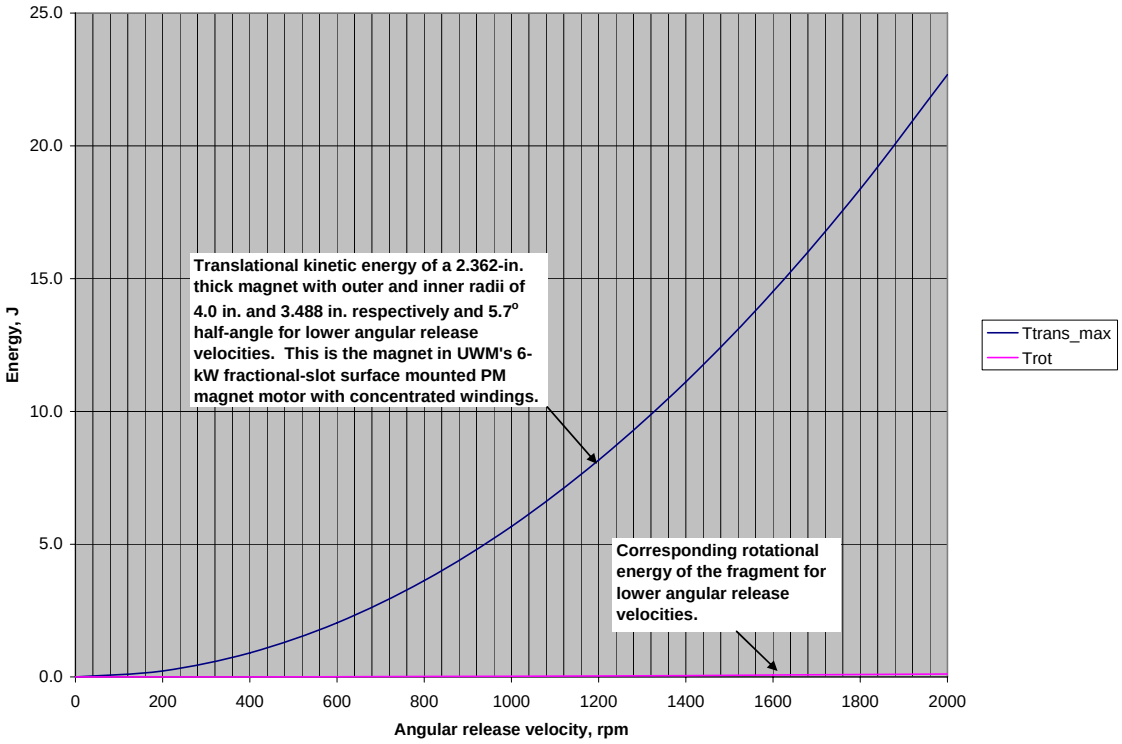

Fig. 4(a). Translational energy of a radial-gap magnet released over a low speed range.

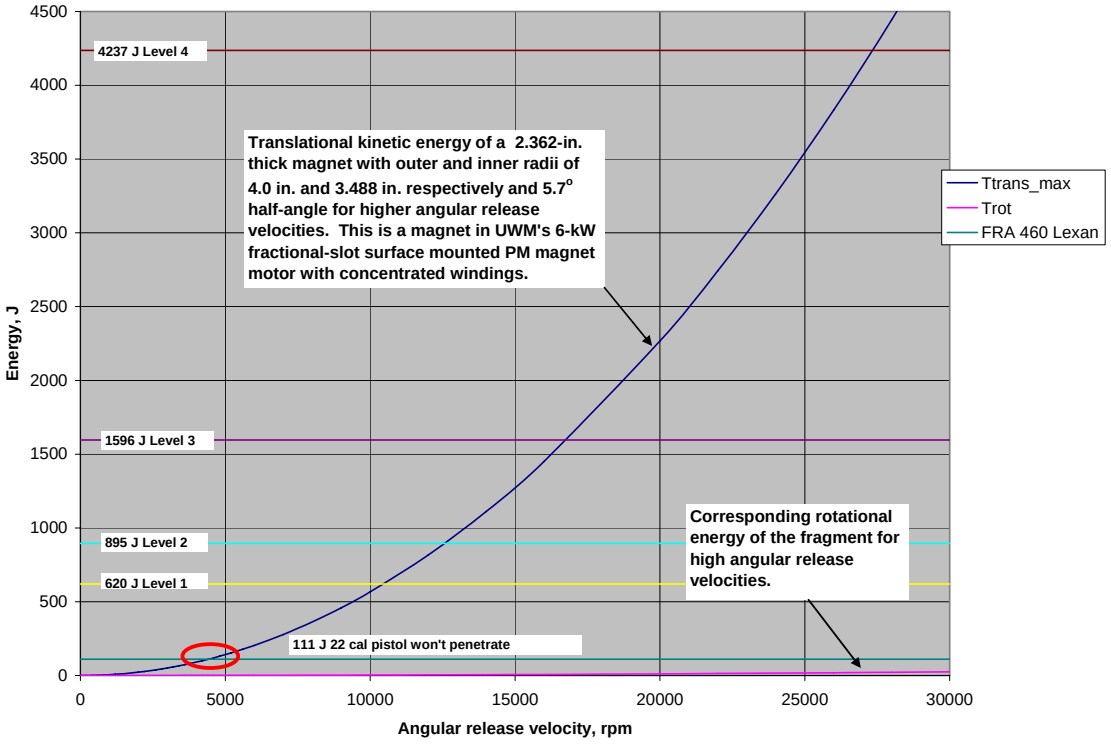

Fig. 4(b). Translational energy of a radial-gap magnet released over a high speed range.

MAXIMUM KINETIC ENERGY CALCULATION FOR A SEGMENT FROM AN ANNULAR ROTOR

In this example, the entire rotor is treated as an annulus that ejects a segment with maximum kinetic energy. The parameters of the annular segment, which acts as a single block, are

ρ is the density of steel, 0.28 $lb_m/in.^3$,

ω is the speed in radians per second ($\omega = \Omega_{rpm} \frac{2\pi}{60}$),

L is the thickness of the ring, 2.67 in.,
R is the outer radius of the annulus, 3.92 in.,
r is the inner radius of the annulus, 3.23 in., and
α is the magnet's half-angle, 66.78173° or 1.165561186 radians.

The upper curve in Fig. 5(a) shows the maximum translational kinetic energy of a segment released from a 50 kW rotor. Its center of mass is moving toward the wall of the enclosure. The curve below it is the corresponding rotational kinetic energy of that fragment about its center of mass. Figure 5(a) is for lower speed analysis. Figure 5(b) is for higher speed analysis.

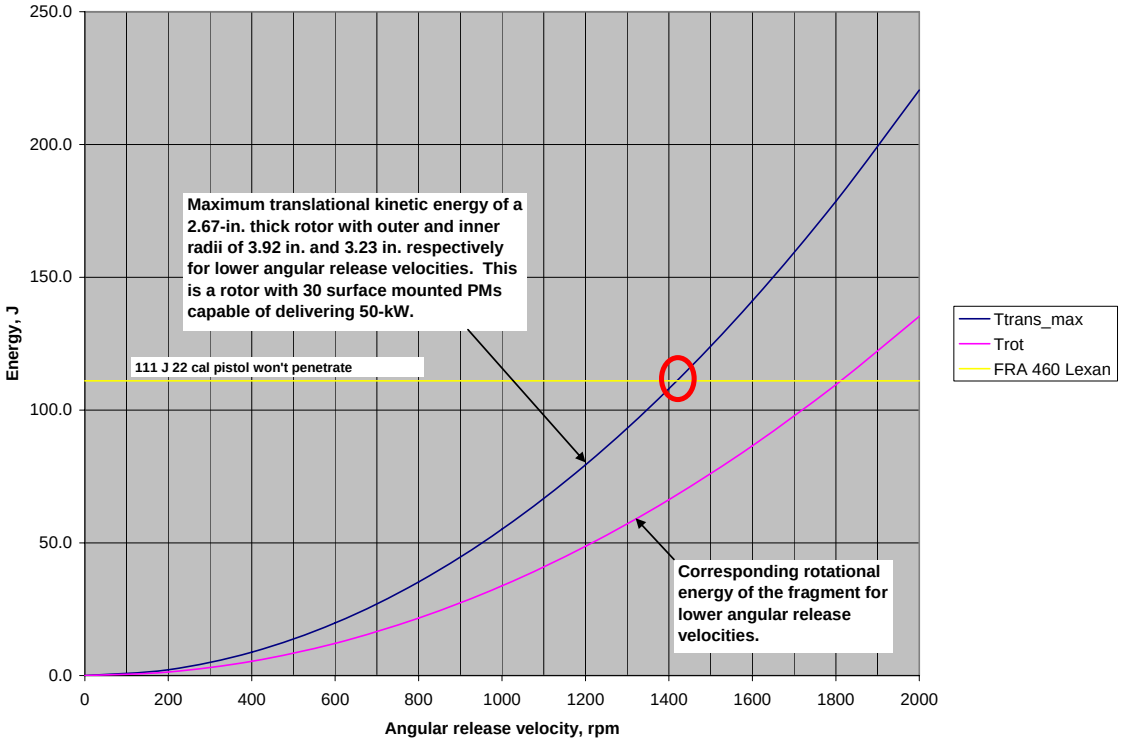

Fig. 5(a). Maximum translational kinetic energy of a rotor segment released over a low speed range.

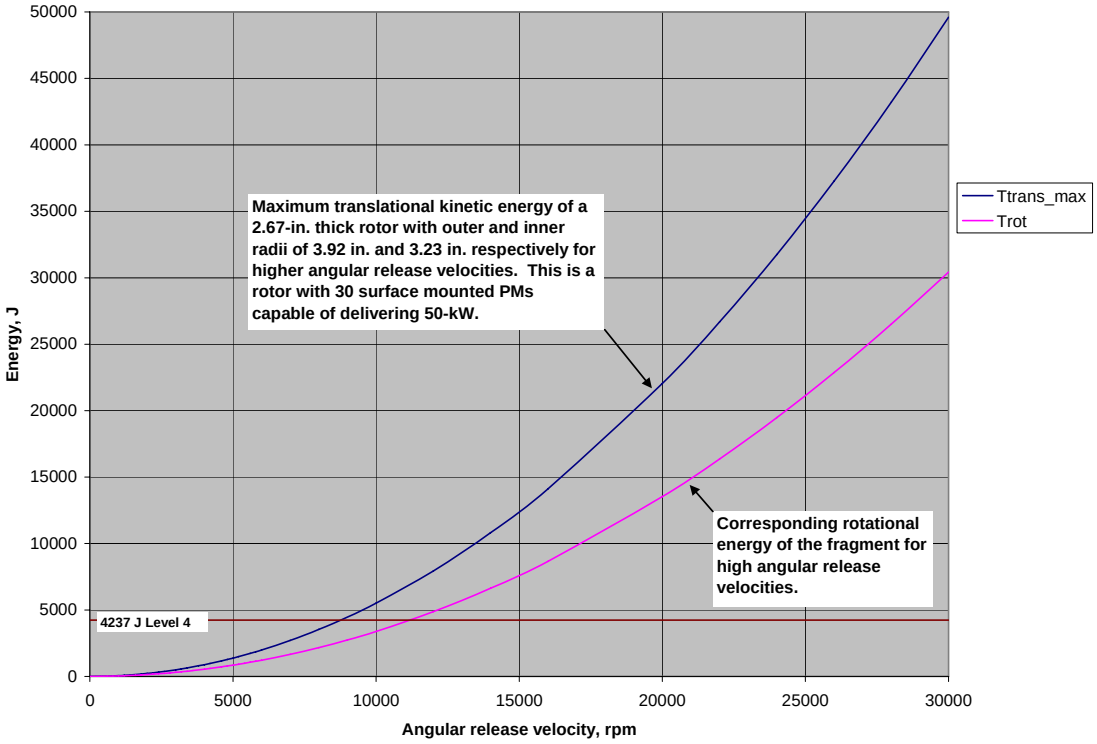

Fig. 5(b). Maximum kinetic energy of a rotor segment released over a high speed range.

When the protection level of a containing material is related to the maximum translational kinetic energy of an ejected fragment from the rotor that must be contained, the maximum permissible rotational speed of that rotor is given by the formula

$$\Omega_{rpm} = 2237\sqrt{\frac{\alpha}{\sin^2(\alpha)}}\sqrt{\frac{\left(1-\left(\frac{r}{R}\right)^2\right)}{\left(1-\left(\frac{r}{R}\right)^3\right)^2}}\frac{1}{R^2}\sqrt{\frac{T}{L}} \quad , \tag{8}$$

where T is the maximum translational kinetic energy, J;
α is the half-angle of the annular segment, radians;
L is the axial dimension of the rotor, in.;
R is the outer radius of the rotor, in.; and
r is the inner radius of the rotor, in.

When a maximum translational kinetic energy fragment occurs, the product of the first two terms on the right of Eq. (8) is 2628. Figure 6 shows that the square root of the Correction Factor, which is the square root of the function of r/R in Eq. (8), may be neglected for values of r/R less than 0.6; consequently a conservative form of Eq. (8) is

$$\Omega_{rpm} = 2628\frac{1}{R^2}\sqrt{\frac{T}{L}} \quad \text{for r/R<0.6 .} \tag{9}$$

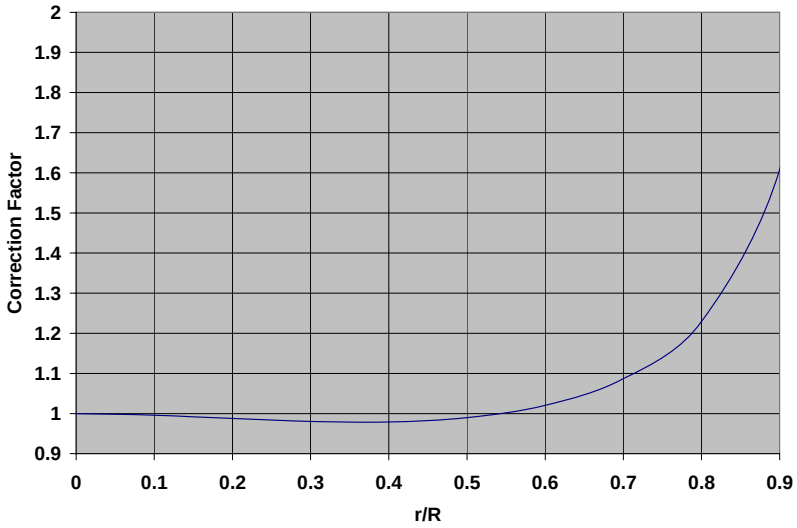

Fig. 6. Correction factor for values of r/R.

Figure 7 shows a plot of Eq. (9) for steel rotor material. The very bottom curve shows the maximum safe conservative speed below which there will not be penetration of a FRA 460 enclosure, which comprises 0.460-in. thick Lexan. It is conservative because the correction factor is ignored. For example, the UWM 6-kW FSCW SPM motor for which $R^2\sqrt{L} = 25.1$ allows conservatively safe operation in an FRA 460 enclosure as long as the motor is operating below 1103 rpm. For this rotor the radius ratio is r/R = 0.824 for which the Correction Factor is 1.286 allowing a 29% increase in safe operating speed; therefore, the maximum safe operating speed is actually 1103*1.286 = 1418 rpm as shown in Fig. 5(a).

When the fragments are magnets instead of maximum translational kinetic energy segments, Eq. (8) may be used with the dimensions of the magnet substituted. The magnet's shape is now given by inner radius, outer radius, length, and half angle of its annular segment.

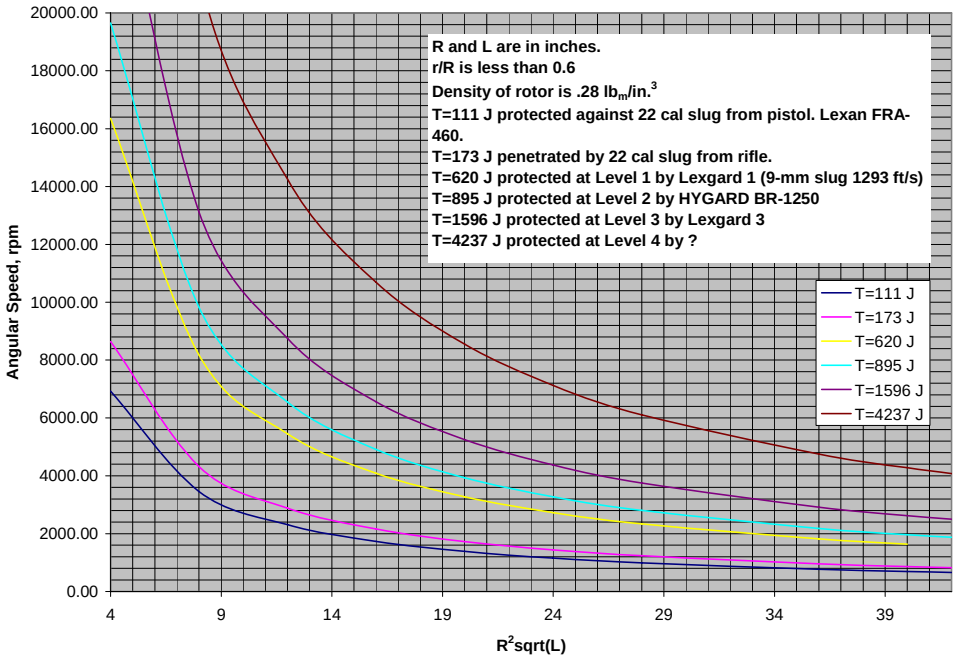

Fig. 7. Proposed safe angular speed for PEEMRC test rotors.

SAFE ACCESS TO TEST CELLS DURING OPERATION

The purpose of this part of the analysis is to determine the maximum rotational speed for permissible entrance into a test cell while a motor is turning. There are times when such entrance is important to hear sounds, take measurements, or modify the test setup.

There are two failure modes, which may be generated during rotor break-up, with the potential to injure an operator in the test cell. The first mode occurs when the rotor releases fragments into the test cell. The fragments might be magnets, which are typically 10–20^{o} segments, or maximum translational kinetic energy segments, which are 133.5^{o} segments of an annular ring. The second mode is failure of the mount system, which may result from either shear of flange bolts on bolt circles concentric to the axis of rotation or tensile fracture of pad mount bolts.

For a representative 55-kW fractional-slot SPM with concentrated windings operating at 20,000 rpm protection from the first mode may be provided by completely enclosing the rotor with a 6061-T6 aluminum housing whose thickness is 0.25-in. or greater. At this speed this motor has 100,000 J of rotational energy. In some cases test rotors, such as the 6-kW fractional-slot SPM rotor with concentrated stator windings are open so that failure fragments can be released directly into the test cell. When the sides of the rotor are open, no access to the test cell during operation is permitted unless the motor is surrounded by a containment fabricated from FRA 460 polycarbonate sheet. The FRA 460 sheet, which is used in railroad car windows, will protect the operator from the equivalent of a 22 caliber slug fired from a pistol. This projectile has energy of 111 J; consequently, the maximum speed for access during operation will be that for which a maximum kinetic energy fragment has no more than 111 J prior to release.

As an example, we apply the 111 J criterion to fragments from two incompletely enclosed PM rotors which have been tested in L002. First, for an open axial-gap PM rotor, the limiting speeds of a maximum translational kinetic energy sector of a titanium support ring and of a magnet from ORNL's axial-gap rotor are 4000 rpm (Fig. 2(b)) and 6000 rpm (Fig. 3(b)). The permissible test cell access speed for the axial-gap motor would be 4000 rpm. For a fractional-slot SPM motor with concentrated windings, the limiting speeds of a magnet and of a maximum translational kinetic energy sector are 4000 rpm (Fig. 4(b)) and 1418 rpm (Fig. 5(a)). The permissible test cell access speed for this set of fragments would be the lower of the two, which is 1418 rpm.

When the motor is completely contained in an aluminum housing the second failure mode, mount failure, must be considered. Mount failure occurs because of torque transferred by the failed rotor fragments to the housing through the stator of a radial-gap motor or directly to the housing by the failed rotor fragments of an axial-gap motor.

The maximum speed for test cell access during operation may be estimated by determining the torque generated during a specific sequence of failure events or by determining the maximum torque that can be sustained by the mount system during failure. There are many sequences of failure events possible and the complex details of most are further complicated by the magnetic properties of the fragments making the first approach time consuming with questionable payoff. Weak link mount analysis is not difficult making the second approach the one that we shall employ.

Application of weak link mount analysis requires two additional assumptions. The first assumption is that all of the reaction of the torque transferred to the housing decelerates the remaining rotor core. In practice some of the torque will generate heat, but this is neglected in this analysis. The second assumption is that the rotor is decelerated to rest in one revolution after the onset of the failure sequence. After one revolution destruction of the rotor should be complete. If the rotor is stopped more rapidly than one revolution, the torque deposited in the housing could be larger. To compensate for these to uncertainties we introduce a safety factor of 5 in the weak link mount analysis.

When failure occurs current will be increased to the motor to maintain its speed quickly leading to an over-current shutoff.

The assumption made in this analysis is that the failure fragments deposit a steady torque, T_{max}, during rubdown and the reaction torque is applied to decelerating the remaining rotor core. The equation for the rubdown time is

$$t_{rd} = \frac{I_p \omega_{init}}{T_{max}} \quad , \tag{10}$$

where ω_{init} is the initial rotational speed, rad/s, and

I_p is the polar moment of inertia of the remaining rotor core, in-lb_f-s^2, which is assumed to be the same as that of the original motor.

This leads to the rubdown angle

$$\theta_{rd} = \omega_{init} t_{rd} - \frac{T_{max}}{I_p} \frac{t_{rd}^2}{2} \quad . \tag{11}$$

The next paragraph will lead to an estimate of T_{max} from the weak link, which is the weakest interface in the mount system, for a 1-revolution rubdown angle.

A representative mount system for Test Cell L003 is shown in Fig. 8. Torque from a rotor breakup is deposited in the housing of the motor on the right and is transferred from the housing to the plate, from the plate to the right flange of the torque meter, from the right flange of the torque meter to the body of the torque meter, from the body of the torque meter to the left flange, from the left flange of the torque meter to the right flange on the gearbox, from the right flange on the gearbox to the body of the gearbox, and from the feet of the gearbox to the aluminum pad. At each of these seven interfaces there are equi-angularly spaced socket head cap screws on a bolt circle whose shear strength can sustain a readily estimated torque. We shall define the test cell access speed during operation for failure mode 2 as the speed at which T_{max} in Eq. (11) is the torque, $T_{sustain}$, which may be sustained by the mount system's weakest interface reduced by a safety factor, *sf*, for a one revolution rubdown angle. This relation, which is $T_{max} = T_{sustain}/sf$, is incorporated into Eq. (11) to obtain the equation for test cell access speed

$$\omega_{initial} = \sqrt{\frac{2\theta_{rd} T_{sustain}}{I_p \cdot sf}} \quad . \tag{12}$$

The weakest interfaces are where eight 10-32 socket head screws hold the flanges of the torque meter to its body. The torque that may be sustained by these bolts about the torque meter's axis is 21,200 in.-lb_f. For the fractional-slot SPM motor with concentrated windings, the value of I_p is 0.38754 lb_f-in.-s^2. The test cell access speed with a safety factor of 5 for a 1-revolution rubdown is 370 rad/s, which corresponds to 3541 rpm. This is 2% below the 3600 rpm operating speed of many commercial industrial electric motors and will serve as the maximum speed for safe access to a completely enclosed electric motor secured with a mount that can sustain 21,200 in-lbf while it is in actual operation in both the lab and test cell at the PEEMRC. If a completely enclosed motor is mounted on a bench with clamps that can sustain less torque, then a lower estimate of the maximum speed for safe access may be made using Eq. 12 with the same safety factor of 5.

To summarize, the maximum permissible access speed during operation for a completely enclosed motor depends upon the lowest torque that may be sustained by the connecting interfaces in the mount system, the polar moment of inertia of the rotor, and an assumed 1 revolution rubdown with a safety factor of 5 to allow for the unknown amount of additional torque that will be applied to the housing as failure fragments are pulverized.

All interface bolts are socket cap screws fabricated from an alloy steel that conforms to ASTM A 574. The tensile strength of this is 170,000 psi, which corresponds to Grade 8 bolt strength. The corresponding shear strength is 85,000 psi. Table 2 summarizes the sustainable torque at the mount interfaces. The tensile stress area of a threaded bolt is

$$A_{tensile} = \frac{\pi}{4}\left(D - \frac{0.9743}{N} \right)^2 \tag{13}$$

where D is the nominal diameter, in., and
N is the number of threads per inch.

Similarly the shear area of a threaded bolt is

$$A_{shear} = \frac{\pi}{4}\left(D - \frac{1.3}{N}\right)^2 \quad . \tag{14}$$

Table 2. Sustainable torque at the mount interfaces in test cell L003

Inter-face	SHS	No. bolts	Type Area	Area, in.^{2}	Bolt circle dia, in.	Torque, in.-lb$_f$.
1	M8-1.25	13	Shear	0.04907	~18	488,000
2,5	3/8-16	6	Shear	0.06777	5	86,400
3,4	10-32	8	Shear	0.01752	3.5625	**21,200**
6	5/16-18	4	Shear	0.04534	4.95	38,154
7	1/2-13	2	Tensile	0.1419	NA	820,000

For each of the flange interfaces the sustainable torque is given by

$$T = n\tau_{shear}A_{shear} \tag{13}$$

where n is the number of bolts, in.
τ_{shear} is the shear strength of the bolt, which is half the tensile strength, 85,000 lb$_f$/in.^{2}, and
A_{shear} is the shear area of the bolt, in.^{2}.

All four 1/2-13 mount bolts extend about 1.3 in. into the aluminum pad. This is 2.5 times deeper more than sufficient to keep them from pulling out during a failure. The torsion sustained by two bolts about a pivot point r_m in. from the center of the bolt as shown in Fig. 1.b. is

$$T_{max} = 2\sigma_{tensile}A_{tensile}r_m + W_{gearbox}r_g \tag{14}$$

where $\sigma_{tensile}$ is the tensile strength of the Grade 8 pad mount bolts, lb$_f$/in.^{2},
$A_{tensile}$ is the tensile area of the pad mount bolts, in.^{2},
r_m is the distance from the pad mount bolts to the opposite base pivot point, in.,
$W_{gearbox}$ is the weight of the gearbox estimated as 300 lb$_f$,
r_g is the lever arm of the gearbox's center of mass, in.

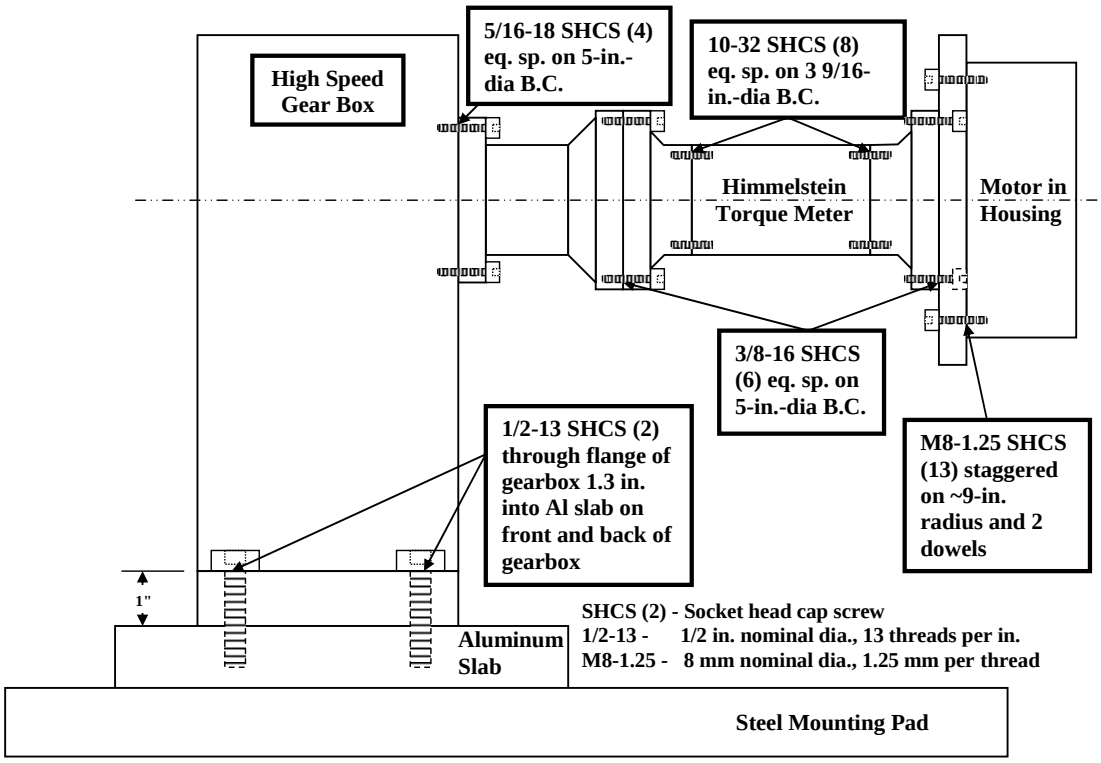

(a) Front view.

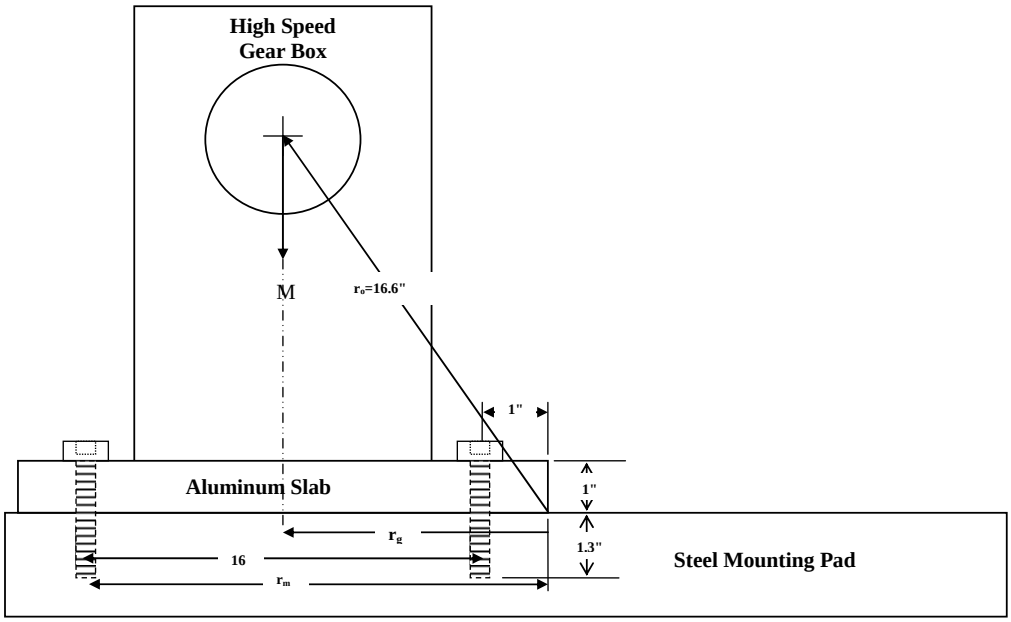

(b) Side view.

Fig. 8. Typical high speed gear box mount system in cell L003.

The torque sustained by the two bolts is 820,000 in.-lb_f with an additional 2,700 in.-lb_f supplied by the weight of the gearbox, which we shall neglect.

The lowest torque is sustained by the eight 10-32 bolts at interfaces 3 and 4 that hold the flanges of the torque meter to its body. They can sustain 21,200 in-lb_f of torque.

CONCLUSIONS

These calculations may be used to estimate what material should be considered for the bullet resistant enclosure to contain typical fragments over given speed ranges.

Two types of bullet resistant materials are Acrylic sheet and polycarbonate laminates. ORNL uses laminated Lexgard® polycarbonate laminates for Level 1 protection by the window in the electric motor test cells. Working with GE the Federal Railway Administration has established that FRA 460, which is 0.460-in. thick Lexan, may be used as window material for passenger cars because it will not be penetrated by a 0.22 caliber slug shot from a pistol with an energy of 111 J.

This information permits operation of a test motor outside a test cell as long as it is enclosed in a box made from FRA 460. Conservative safe operating speed against penetration by a 133° segment of a 55-kW FSCW motor is 1103 rpm. When the correction factor is applied for r/R = 0.824, a 29% increase is allowed in the safe operating speed, which leads to the 1418 rpm value shown in Fig. 5(a).

When the motor is completely contained in an aluminum housing the second failure mode, mount failure, must be considered. Mount failure occurs because of torque transferred by the failed rotor fragments to the housing through the stator of a radial-gap motor or directly to the housing by the failed rotor fragments of an axial-gap motor.

The maximum speed for test cell access during operation may be estimated by determining the torque generated during a specific sequence of failure events or by determining the maximum torque that can be sustained by the mount system during failure at its weakest interface or weak link. Application of weak link mount analysis requires two additional assumptions. The first assumption is that all of the reaction of the torque transferred to the housing decelerates the remaining rotor core. In practice some of the torque will generate heat, but this is neglected in this analysis. The second assumption is that the rotor is decelerated to rest in one revolution after the onset of the failure sequence. After one revolution destruction of the rotor should be complete. If the rotor is stopped more rapidly than one revolution, the torque deposited in the housing could be larger. To compensate for these two uncertainties we introduce a safety factor of 5 in the weak link mount analysis. This approach leads to a maximum access during operation speed of 3541 rpm for a completely enclosed PM motor.

REFERENCES

1. *Underwriters Laboratory UL 752 Standard Bullet Resisting Equipment*, Ninth Edition, September 27, 2005.
2. "Federal Railroad Administration, Department of Transportation, Part 223 Safety Glazing Standards – Locomotives, Passenger Cards, and Cabooses,"*49 CFR Transportation*, Chapter II.

DISTRIBUTION

Internal

1. D. J. Adams
2. C. L. Coomer
3. J. Czachowski
4. K. P. Gambrell
5. E. C. Fox
6. L. D. Marlino
7. J. W. McKeever
8. M. Olszewski
9. Laboratory Records